Cell Reports, Volume *33*

Supplemental Information

PD-L1 Reverse Signaling in Dermal Dendritic Cells Promotes Dendritic Cell Migration Required for Skin Immunity

Erin D. Lucas, Johnathon B. Schafer, Jennifer Matsuda, Madison Kraus, Matthew A. Burchill, and Beth A. Jirón Tamburini

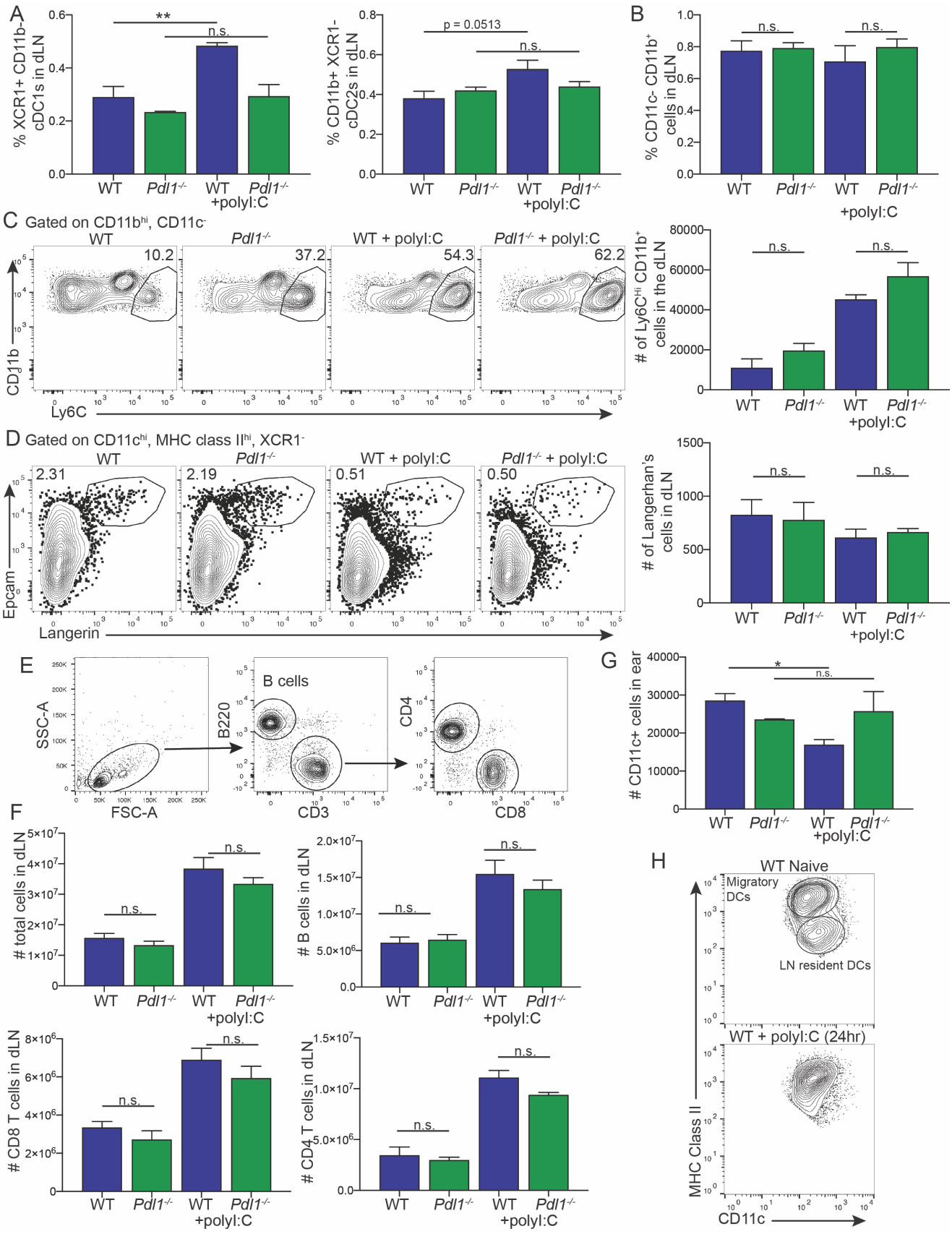
A
% XCR1+ CD11b- cDC1s in dLN
**
n.s.
% CD11b+ XCR1- cDC2s in dLN
p = 0.0513
n.s.
B
% CD11c- CD11b+ cells in dLN
n.s.
n.s.
WT
Pdl1-/-
WT +polyI:C
Pdl1-/- +polyI:C
C Gated on CD11bhi, CD11c-
10.2
37.2
54.3
62.2
CD11b
Ly6C
# of Ly6CHi CD11b+ cells in the dLN
D Gated on CD11chi, MHC class IIhi, XCR1-
2.31
2.19
0.51
0.50
Epcam
Langerin
# of Langerhan's cells in dLN
E
SSC-A
FSC-A
B cells
B220
CD3
CD4
CD8
F
total cells in dLN
B cells in dLN
CD8 T cells in dLN
CD4 T cells in dLN
G
CD11c+ cells in ear
*
H
WT Naive
Migratory DCs
LN resident DCs
WT + polyI:C (24hr)
MHC Class II
CD11c

Figure S1: DCs but not other immune cells are decreased in the dLN in *Pdl1*$^{-/-}$ mice in response to polyI:C. **Related to Figure 1.** A) The percent of total cells in the dLN that are cDC1 and cDC2 at baseline and 24 hours following polyI:C in indicated strain. B) The percent of total cells in the dLN that are CD11c^{-} CD11b^{+} at baseline and 24 hours following polyI:C. C) Representative flow plots and quantification of monocytes (gated on B220^{-}, CD11b^{+} CD11c^{-} as in Figure 1A, then on Ly6C^{hi} cells) in the dLN at baseline and 24 hours following polyI:C injection. D) Representative flow plots and quantification of Langerhans' cells (gated as B220^{-}; MHC class II^{hi}, CD11c^{hi}, XCR1^{-} as in Figure 1A, then on langerin^{+}, Epcam^{+}) in the dLN at baseline and 24 hours following polyI:C injection. E) Gating strategy for B cells, CD4 T cells and CD8 T cells in the dLN. F) The number (#) of total cells, total CD8 T cells, CD4 T cells and B cells in the LN of the WT and *Pdl1*$^{-/-}$ mice at baseline and 24 hours following polyI:C. G) Quantification of total DCs in the ears of mice 24hours following polyI:C injection into the ear. H) Representative flow plots of MHC class II and CD11c expression on total DCs at steady state and 24 hours following polyI:C injection. For A-F data combined from axillary and brachial LNs, n=3 mice per group. Experiment repeated a total of two times with similar results. Statistical analysis was done using a 1-way Anova. *, $P < 0.05$; **, $P < 0.01$. All error bars are standard error of the mean.

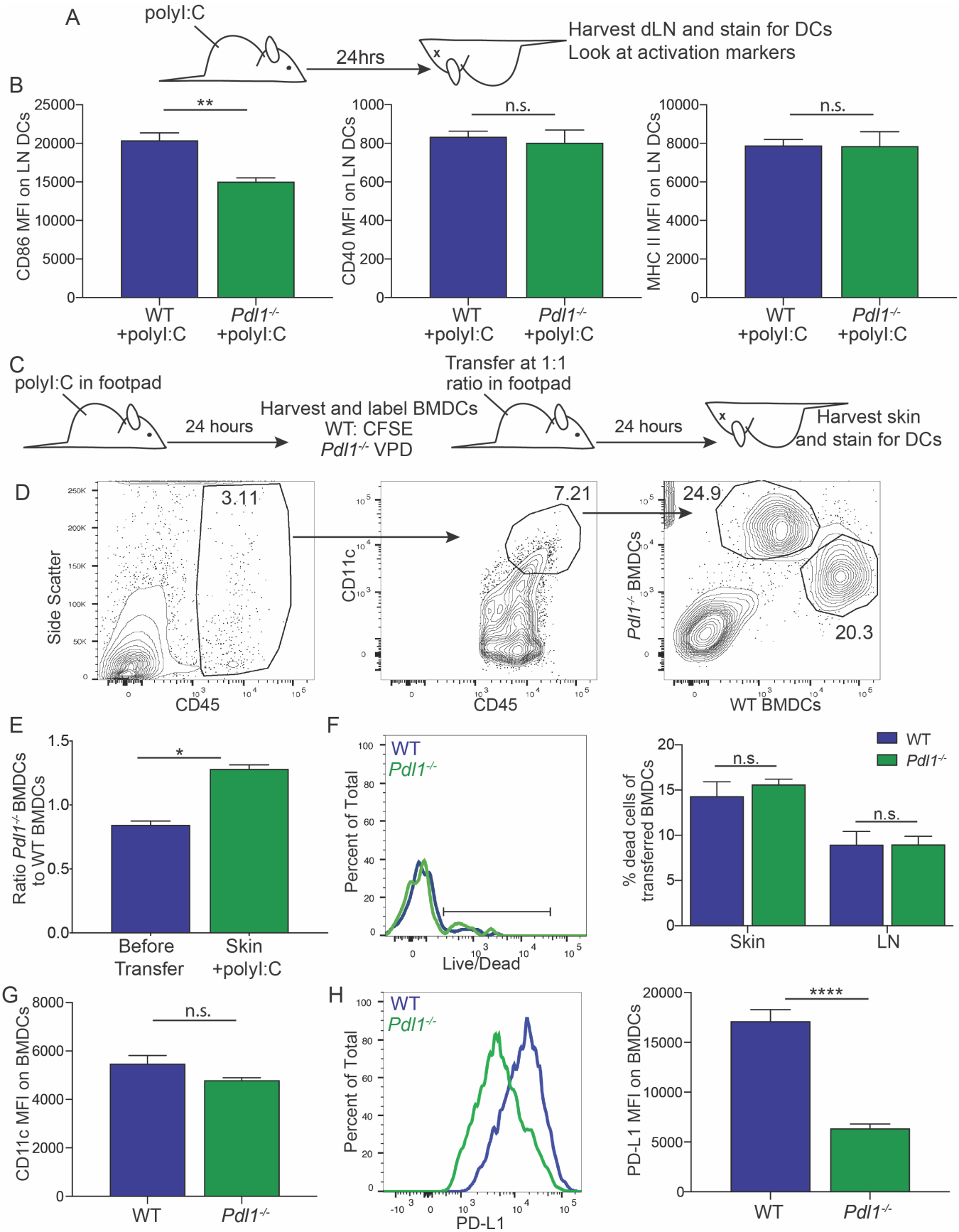
A
polyI:C
24hrs
Harvest dLN and stain for DCs
Look at activation markers
B
CD86 MFI on LN DCs
**
WT +polyI:C
Pdl1-/- +polyI:C
CD40 MFI on LN DCs
n.s.
MHC II MFI on LN DCs
n.s.
C
polyI:C in footpad
24 hours
Harvest and label BMDCs
WT: CFSE
Pdl1-/- VPD
Transfer at 1:1 ratio in footpad
24 hours
Harvest skin and stain for DCs
D
Side Scatter
CD45
3.11
CD11c
7.21
Pdl1-/- BMDCs
WT BMDCs
24.9
20.3
E
Ratio Pdl1-/- BMDCs to WT BMDCs
*
Before Transfer
Skin +polyI:C
F
WT
Pdl1-/-
Percent of Total
Live/Dead
% dead cells of transferred BMDCs
n.s.
n.s.
Skin
LN
G
CD11c MFI on BMDCs
n.s.
WT
Pdl1-/-
H
WT
Pdl1-/-
Percent of Total
PD-L1
PD-L1 MFI on BMDCs
****
WT
Pdl1-/-

Figure S2: Characterization of DC surface markers in the *Pdl1*$^{-/-}$ mouse. Related to Figure 2.
A) Experimental design for B. B) Surface expression of CD86, CD40 and MHC class II on WT and *Pdl1*$^{-/-}$ LN DCs 24 hours following polyI:C. Data combined from axillary and brachial LNs, n=3 mice per group. Repeated three times with similar results. C) Experimental design for D-F. D) Gating strategy and representative flow plots of skin where BMDCs were transferred. E) Ratio of *Pdl1*$^{-/-}$ to WT BMDCs recovered from the injection site following transfer into mice. Data shown from skin at site of BMDC transfer, n=3 mice per group. Repeated three times with similar results. F) Representative flow plot from dLN and quantification of transferred BMDCs stained with a live/dead marker (Ghost Dye Red 780). Quantification shown from injection site of the skin and the dLN. n=3 mice per group. G) CD11c surface expression on WT and *Pdl1*$^{-/-}$ BMDCs following activation with LPS (200ng/mL, 4hrs). H) Representative flow plot and quantification of PD-L1 surface expression WT and *Pdl1*$^{-/-}$ BMDCs following activation with LPS (200ng/mL, 4hrs). Data in G and H shown from 3 technical replicates per group, experiment repeated three times with similar results. Statistical analysis was done using an unpaired student's t test. *, $P< 0.05$; **, $P < 0.01$; ****, $P < 0.0001$. All error bars are standard error of the mean.

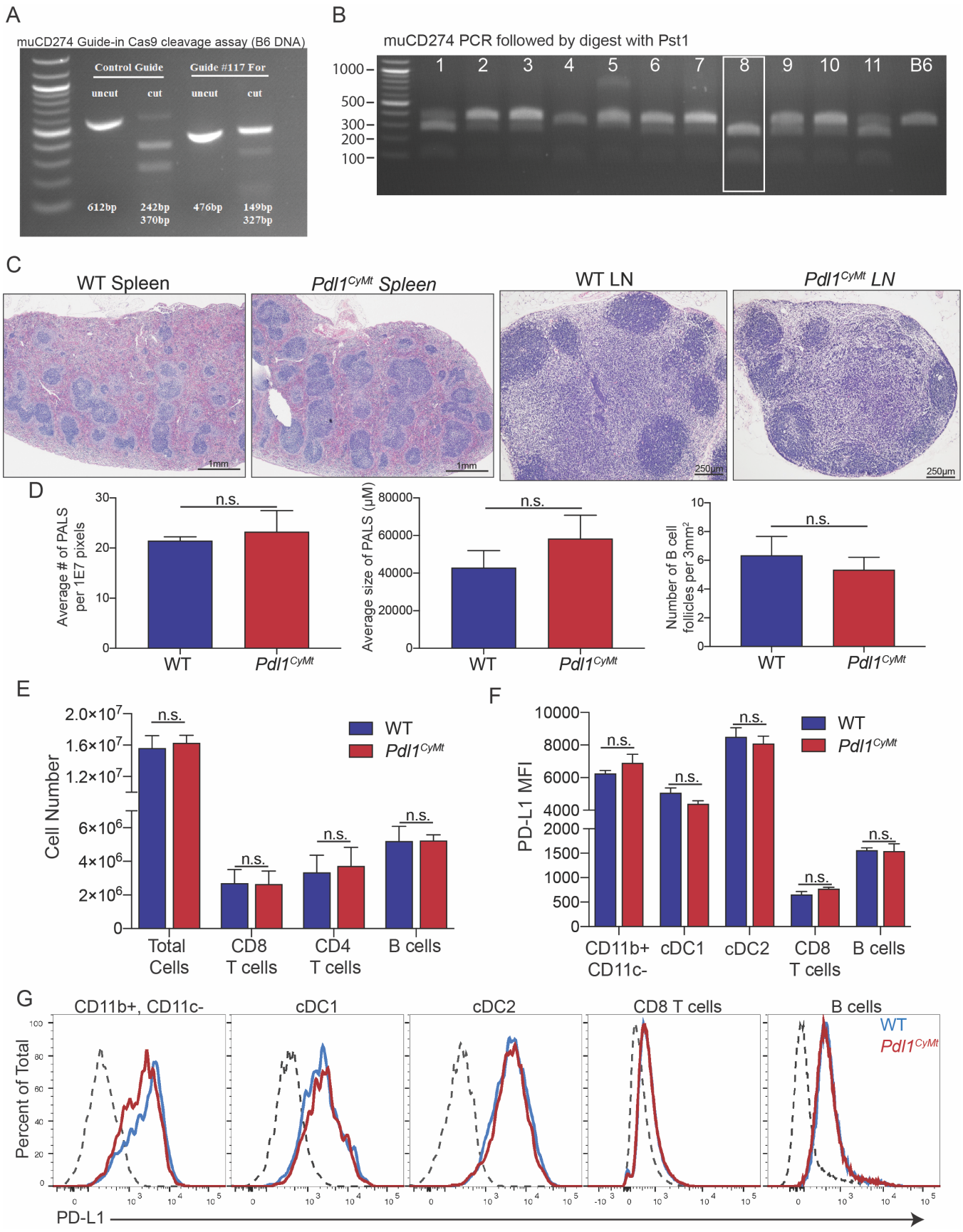
A
muCD274 Guide-in Cas9 cleavage assay (B6 DNA)
Control Guide
Guide #117 For
uncut
cut
uncut
cut
612bp
242bp
370bp
476bp
149bp
327bp
B
muCD274 PCR followed by digest with Pst1
1000
500
300
200
100
1
2
3
4
5
6
7
8
9
10
11
B6
C
WT Spleen
Pdl1CyMt Spleen
WT LN
Pdl1CyMt LN
1mm
1mm
250μm
250μm
D
Average # of PALS per 1E7 pixels
n.s.
WT
Pdl1CyMt
Average size of PALS (μM)
n.s.
WT
Pdl1CyMt
Number of B cell follicles per 3mm2
n.s.
WT
Pdl1CyMt
E
Cell Number
n.s.
WT
Pdl1CyMt
Total Cells
CD8 T cells
CD4 T cells
B cells
F
PD-L1 MFI
WT
Pdl1CyMt
CD11b+ CD11c-
cDC1
cDC2
CD8 T cells
B cells
G
CD11b+, CD11c-
cDC1
cDC2
CD8 T cells
B cells
WT
Pdl1CyMt
Percent of Total
PD-L1

Figure S3: Characterization of the immune tissue in the *Pdl1*^{CyMt} mouse. Related to Figure 3. A) Incubation of guide RNA and Cas9 protein with PCR product containing the target sequence. Confirmation of guide activity by comparison to a positive "control guide" known to cut and produce cleavage products at 242bp and 370bp and our selected guide #117 which produced products at 149 and 327 base pairs. B) The digest with Pst1 showing a 149bp and 327 bp product where the mutation was successfully introduced and a 476 bp product showing the WT band. Number 8 appears homozygous for the mutation and was selected for breeding. C) Representative images showing H&E microscopy of spleens (left)s and skin draining LNs (right) from WT and *Pdl1*^{CyMt} mice. D) Quantification of periarterial lymphatic sheaths (PALs) showing number and size in the spleens, and number of B cell follicles in LNs of WT and *Pdl1*^{CyMt} mice. E) Quantification of cell numbers by flow cytometry from skin draining LNs of *Pdl1*^{CyMt} mice, derived from Founder 8 compared, to WT mice. F) Quantification of PD-L1 surface expression by flow cytometry of indicated cells from skin draining LNs of *Pdl1*^{CyMt} mice derived from Founder 8 compared to WT mice. G) Representative flow plots of PD-L1 expression quantified in Figure S3F. Dotted line is *Pdl1*$^{-/-}$ control for no expression. For E-G data shown from axillary and brachial LNs, n=3 mice each in data shown, repeated a total of three times with similar results. None of the values were significant between WT and *Pdl1*^{CyMt} mice as assessed by a student's t-test. All error bars are standard error of the mean.

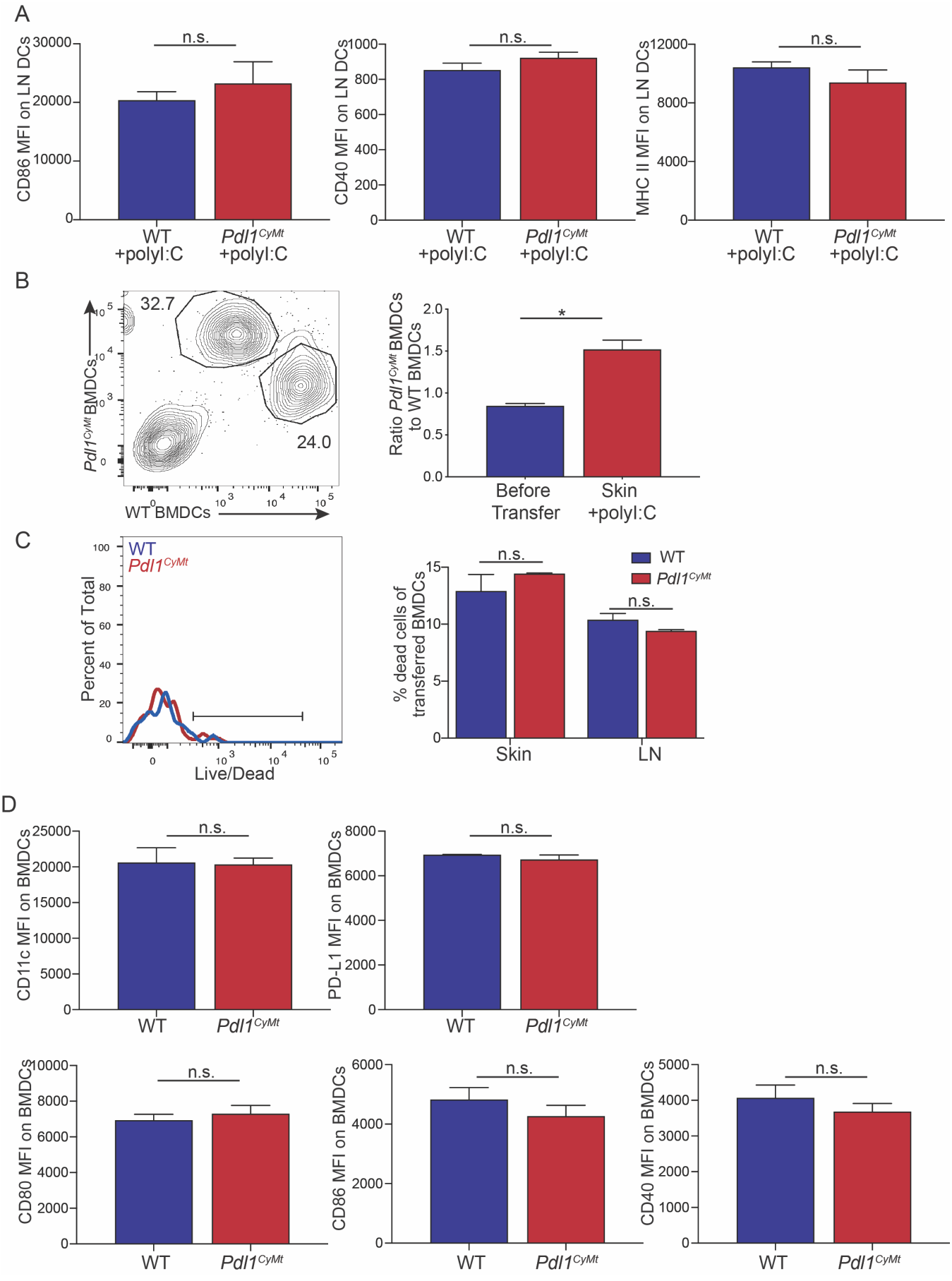
A
CD86 MFI on LN DCs
n.s.
WT +polyI:C
Pdl1CyMt +polyI:C
CD40 MFI on LN DCs
MHC II MFI on LN DCs
B
32.7
24.0
Pdl1CyMt BMDCs
WT BMDCs
Ratio Pdl1CyMt BMDCs to WT BMDCs
*
Before Transfer
Skin +polyI:C
C
WT
Pdl1CyMt
Percent of Total
Live/Dead
% dead cells of transferred BMDCs
Skin
LN
D
CD11c MFI on BMDCs
PD-L1 MFI on BMDCs
CD80 MFI on BMDCs
CD86 MFI on BMDCs
CD40 MFI on BMDCs

Figure S4: Characterization of DC surface markers in the *Pdl1*^{CyMt} mouse. Related to Figure 3. A) Surface expression of CD86, CD40 and MHC class II on WT and *Pdl1*^{CyMt} LN DCs 24 hours following polyI:C. Data shown from axillary and brachial LNs, n=3 mice per group, experiments repeated two-three times total. B) Representative flow plots and quantification showing the ratio of *Pdl1*^{CyMt} to WT BMDCs recovered from the injection site following transfer into mice. Data shown from ear taken after BMDC transfer, n=3 mice per group. Repeated three times with similar results. C) Representative flow plot from dLN and quantification of transferred BMDCs stained with a live/dead marker (Ghost Dye Red 780). Quantification shown from injection site of the skin and the dLN. n=3 mice per group. D) CD11c, PD-L1, CD80, CD86 and CD40 surface expression on WT and *Pdl1*^{CyMt} BMDCs following activation with LPS (200ng/mL, 4hrs). Data shown from 3 technical replicates per group, experiment repeated three times with similar results. Statistical analysis was done using an unpaired student's t test. *, $P < 0.05$ All error bars are standard error of the mean.

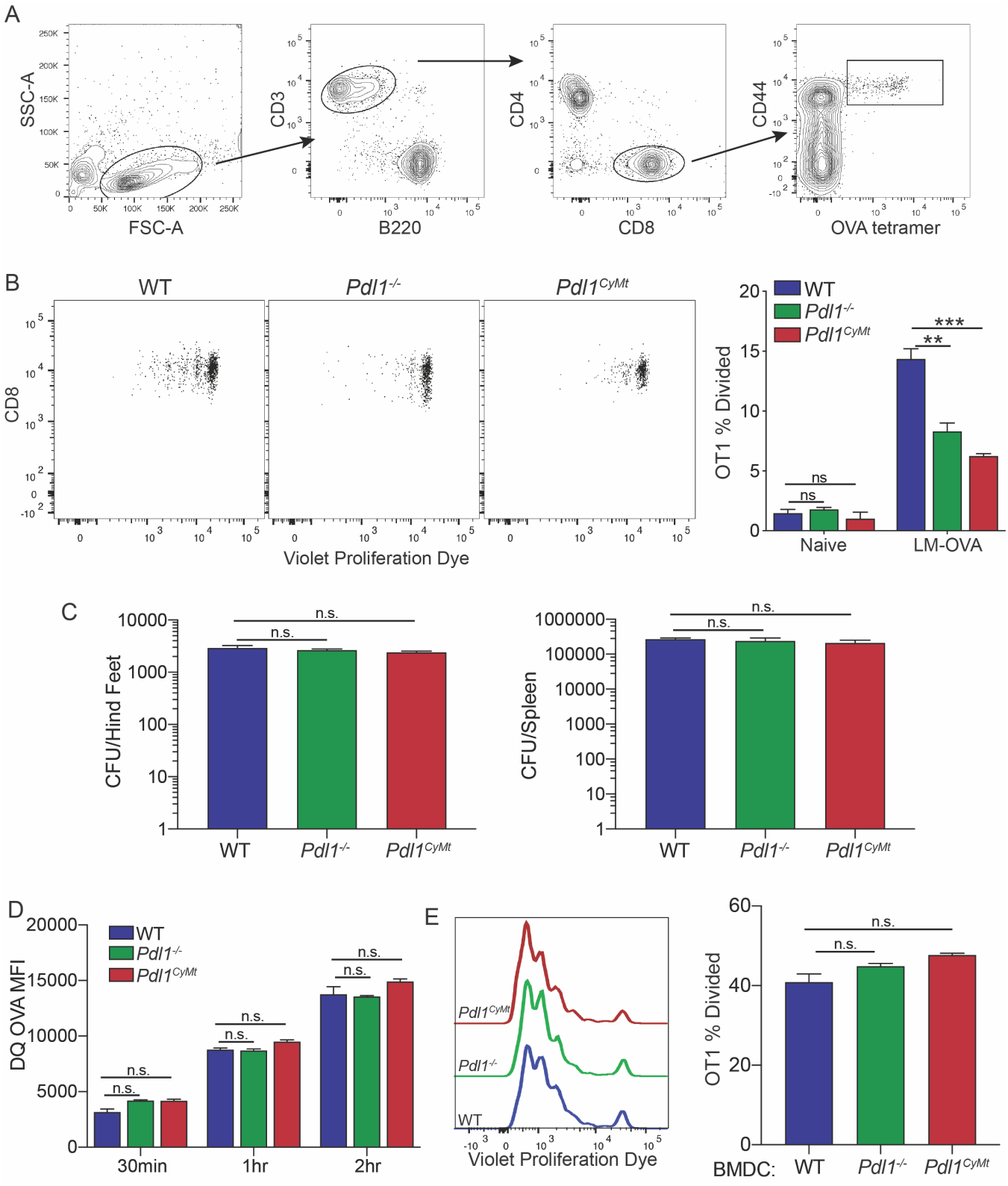
A
SSC-A
FSC-A
CD3
B220
CD4
CD8
CD44
OVA tetramer
B
WT
Pdl1-/-
Pdl1CyMt
CD8
Violet Proliferation Dye
OT1 % Divided
ns
ns
**
***
Naive
LM-OVA
C
CFU/Hind Feet
CFU/Spleen
n.s.
WT
Pdl1-/-
Pdl1CyMt
D
DQ OVA MFI
30min
1hr
2hr
E
Violet Proliferation Dye
OT1 % Divided
BMDC:

Figure S5: Defects in T cells responses are not T cell intrinsic or due to loss of antigen processing or presentation. Related to Figure 4. A) Gating strategy for H2Kb SIINFEKL specific tetramer+ T cells (OVA specific T cells). Cells were gated as CD3+, B220-, CD8+, $CD44^{hi}$ and OVA tetramer+. B) Representative flow plots and quantification of transferred Violet Proliferation Dye labeled WT OT1s. Percent divided was calculated from popliteal LNs 4 days following transfer into mice infected with LM-OVA (1e3 CFU/footpad). Data shown from two combined experiments, n=3-6 mice per group. C) LM-ova CFU from hind feet and spleen of infected mice three days following infection in the hind footpad or intravenous injection. n=3 mice per group. D) Quantification of DQ-OVA fluorescence at indicated times of incubation. Fluorescence of BMDCs incubated with DQ-OVA for 2 hours on ice was subtracted. Data shown with n=5-7 technical replicates per group. E) Representative flow plots and quantification of OT1 division following 3 days of co-culture with WT, *Pdl1*$^{-/-}$ or *Pdl1*^{CyMt} BMDCs. BMDCs were treated with OVA (25μg/mL), polyI:C (12.5μg/mL) and αCD40 (12.5μg/mL) for 24hrs prior to co-culture. Cells were cultured at a 10:1 ratio of OT1 T cells to BMDCs from indicated mouse strain. Data shown with n=7 technical replicates per group. Statistical analysis was done using a 1-way Anova. **, $P < 0.01$; ***, $P < 0.001$. All error bars are standard error of the mean.

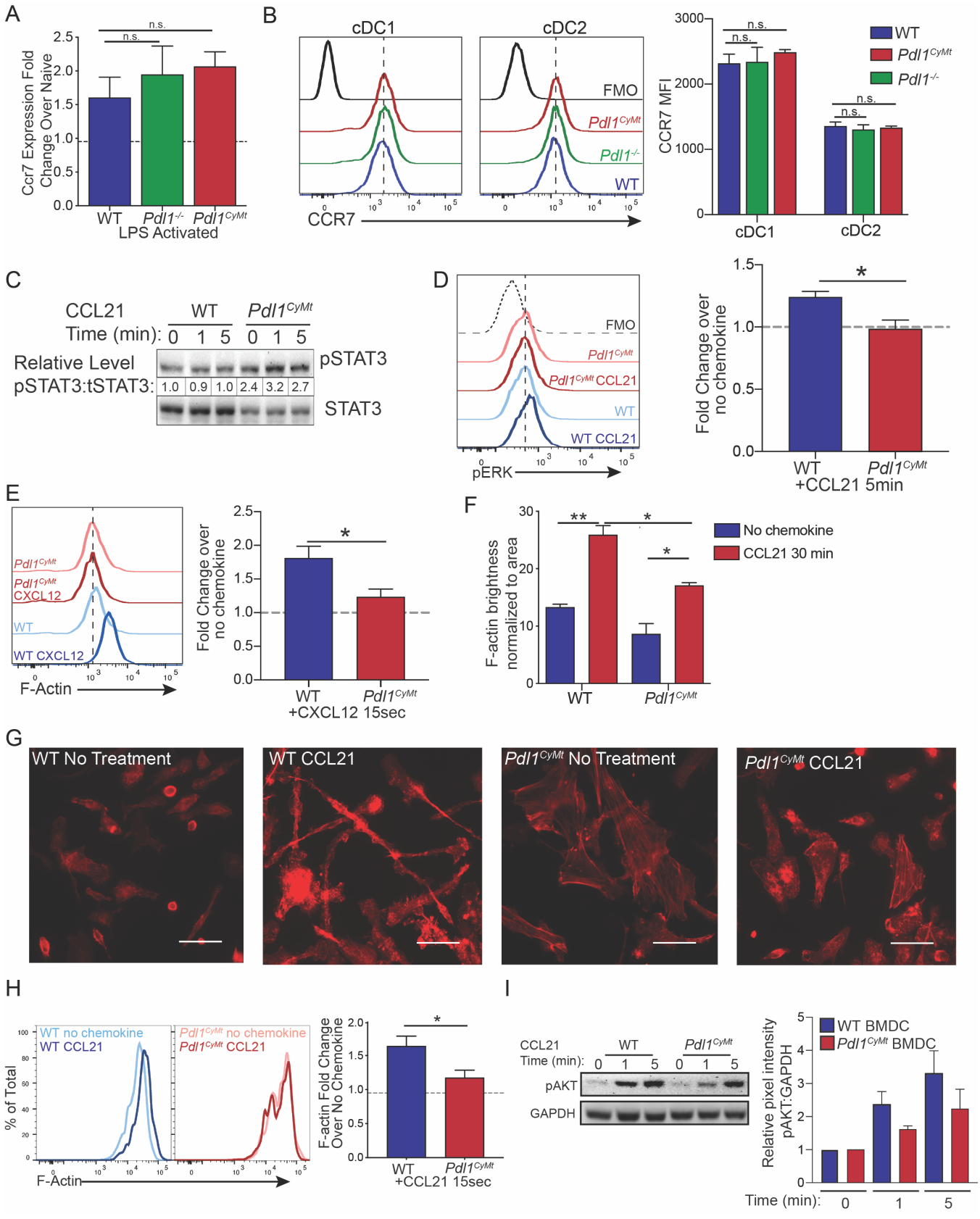
A
Ccr7 Expression Fold Change Over Naive
n.s.
n.s.
WT
Pdl1-/-
Pdl1CyMt
LPS Activated
B
cDC1
cDC2
FMO
Pdl1CyMt
Pdl1-/-
WT
CCR7
CCR7 MFI
n.s.
n.s.
n.s.
n.s.
WT
Pdl1CyMt
Pdl1-/-
cDC1
cDC2
C
CCL21
Time (min): 0 1 5 0 1 5
WT
Pdl1CyMt
Relative Level
pSTAT3:tSTAT3:
1.0 0.9 1.0 2.4 3.2 2.7
pSTAT3
STAT3
D
FMO
Pdl1CyMt
Pdl1CyMt CCL21
WT
WT CCL21
pERK
Fold Change over no chemokine
*
WT
Pdl1CyMt
+CCL21 5min
E
Pdl1CyMt
Pdl1CyMt CXCL12
WT
WT CXCL12
F-Actin
Fold Change over no chemokine
*
WT
Pdl1CyMt
+CXCL12 15sec
F
F-actin brightness normalized to area
**
*
*
No chemokine
CCL21 30 min
WT
Pdl1CyMt
G
WT No Treatment
WT CCL21
Pdl1CyMt No Treatment
Pdl1CyMt CCL21
H
WT no chemokine
WT CCL21
Pdl1CyMt no chemokine
Pdl1CyMt CCL21
% of Total
F-Actin
F-actin Fold Change Over No Chemokine
*
WT
Pdl1CyMt
+CCL21 15sec
I
CCL21
Time (min): 0 1 5 0 1 5
WT
Pdl1CyMt
pAKT
GAPDH
Relative pixel intensity pAKT:GAPDH
WT BMDC
Pdl1CyMt BMDC
Time (min): 0 1 5

Figure S6: **Loss of PD-L1 signaling impairs chemokine responses in BMDCs. Related to Figure 5 and Figure 6.** A) RT-qPCR expression of Ccr7 on LPS activated BMDCs. Results shown as fold-change in transcrip over WT naïve BMDC. Dashed line indicates WT naïve. n=3 technical replicates per group. Experiment was repeated a total of three times with similar results. B) Representative flow plots and quantification of CCR7 mean fluoresce intensity (MFI) on LN cDC1 and cDC2. C) Western blot image and quantification using antibodies against STAT3 and pSTAT3 at 0, 1 or 5 minutes following CCL21 (1μg/mL) in BMDCs. The ratio of pSTAT3 to STAT3 was calculated and all differences shown as relative to WT at time zero. D) Representative flow plots and quantification of phosphorylated ERK to total ERK shown at time zero compared to time 5 minutes. n=2-3 three technical replicates per group. Data shown from two independent experiments. E) Representative flow plots and quantification of F-actin polymerization in BMDCs following 15 sec of CXCL12 treatment (1μg/mL). n=3 replicates per group, experiment repeated a total of two times with similar results. F) Quantification of G showing fold change in F-actin brightness over no chemokine G) Representative images of phalloidin staining on BMDCs 30min following treatment with CCL21 (1μg/mL). Data shown with 3 technical replicates per group. Experiment was repeated twice with similar results. H) Representative flow plots and quantification of F-actin polymerization in LN DCs following 15 sec of CCL21 treatment (1μg/mL). n=3-4 mice per group. Data shown combined from two independent groups. I) Western blot image and quantification using antibodies against p-AKT and GAPDH at 0, 1 or 5 minutes following CCL21 (1μg/mL) addition to BMDC media. Experiment was repeated twice with similar results. Statistical analysis was done using a 1-way Anova (A,C) or an unpaired student's t test (D-I). *, $P< 0.05$; **, $P < 0.01$; ***, $P < 0.001$; ****, $P < 0.0001$. All error bars are standard error of the mean.

Sites screened for off target mutations	Sequence
Off Target Site 1: chromosome 12, intergenic: Rad51b-Zfp36l1/Gm26669	CCAACCTCAGAAAACAGAAA
Off Target Site 2: chromosome 10, intron: Sim1	AAAAACAAAAAAAACCGAAA
Off Target Site 3 chromosome X, intron: Pola1	GGAAGCTCAAAAAGCAGAAA
Off Target Site 4: chromosome 12, intergenic: Slc10a1-Smoc1	TTTTTGTTTTTTAAGATTGT
Off Target Site 5: chromosome 16, intron: Nrip1	CCAACCTCAGAAACAGAAA

Table S1: Off Target Site Sequencing Results. Related to Figure 3 and Figure S3. Locations and sequences of the five putative off-target sites following CRISPR-Cas9 mediated mutagenesis for the mutation in the Pdl1^{CyMt} mouse strain.